Annual Review of Physical Chemistry

Lipid Landscapes: Vibrational Spectroscopy for Decoding Membrane Complexity

Xiaobing Chen, Ziareena A. Al-Mualem, and Carlos R. Baiz

Department of Chemistry, University of Texas at Austin, Austin, Texas, USA;
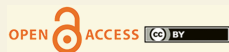email: cbaiz@cm.utexas.edu

ANNUAL REVIEWS CONNECT

www.annualreviews.org

- Download figures
- Navigate cited references
- Keyword search
- Explore related articles
- Share via email or social media

Keywords

lipids, spectroscopy, membranes, infrared, vibrational, ultrafast, SEIRAS, 2D IR

Abstract

Cell membranes are incredibly complex environments containing hundreds of components. Despite substantial advances in the past decade, fundamental questions related to lipid-lipid interactions and heterogeneity persist. This review explores the complexity of lipid membranes, showcasing recent advances in vibrational spectroscopy to characterize the structure, dynamics, and interactions at the membrane interface. We include an overview of modern techniques such as surface-enhanced infrared spectroscopy as a steady-state technique with single-bilayer sensitivity, two-dimensional sum-frequency generation spectroscopy, and two-dimensional infrared spectroscopy to measure time-evolving structures and dynamics with femtosecond time resolution. Furthermore, we discuss the potential of multiscale molecular dynamics (MD) simulations, focusing on recently developed simulation algorithms, which have emerged as a powerful approach to interpret complex spectra. We highlight the ongoing challenges in studying heterogeneous environments in multicomponent membranes via current vibrational spectroscopic techniques and MD simulations. Overall, this review provides an up-to-date comprehensive overview of the powerful combination of vibrational spectroscopy and simulations, which has great potential to illuminate lipid-lipid, lipid-protein, and lipid-water interactions in the intricate conformational landscape of cell membranes.

1. INTRODUCTION

1.1. A Century of Membrane Models

Fluid-mosaic model:
an influential
membrane model
consisting of proteins
embedded within the
lipid bilayer

Order and structure at every length scale are some of the hallmarks of biology. Lipid membranes provide molecular-scale barriers that compartmentalize a cell's internal components as well as separate the delicate machinery of the cell from its surroundings. Their structure and physical, chemical, and mechanical properties support the multiple roles of membranes, including as a physical barrier to support concentration gradients in energy production, as well as signaling, sensing, and transport (1–6). While the biochemical properties of membranes were relatively well established in early studies, the structure and composition were difficult to characterize, mainly due to a lack of experimental techniques that could provide molecular-level structure, a task that remains challenging to this day. The original bilayer idea was first proposed in 1925, based on area-per-lipid measurements of compositions extracted from mammalian cells (7, 8). Later, in the mid-1930s, Davson and Danielli proposed the first molecular model that incorporated proteins as part of the plasma membrane (9). The model was informed by early measurements of differential permeabilities, electron microscopy, thermodynamic properties such as the phase transition temperature, and, new at the time, X-ray investigations of protein crystals that showed dense cores solvated by water (10). Since proteins were known to be solvated by water at the time, a sandwich-like structure was proposed (**Figure 1a**). In this model, a porous protein film would be located above and below the bilayer. While this model is too crude by current standards, it incorporates some key elements that we associate with cell membranes. In addition, despite the simplistic models, the importance of hydrogen-bonding and lipid-lipid interactions was recognized early on, and infrared (IR) spectroscopy, among other techniques, played an important role in supporting a dynamic fluid-like bilayer view that we still associate with cell membranes today (11, 12).

The more influential fluid-mosaic model was developed in the 1970s by Singer & Nicolson (13) (**Figure 1b**). Within this picture, membrane proteins are arranged in oriented amphipathic structures partially embedded within the phospholipid matrix, which is organized as a continuous fluid bilayer. This was based on X-ray crystallography, freeze-fracture electron microscopy, bulk thermodynamic measurements, and other biochemical studies. While this model has obvious limitations, the basic concept of transmembrane proteins embedded within the bulk bilayer is sufficient to explain many observations, and thus, the fluid-mosaic model remains relevant as a qualitative description of the local membrane environment (14). Initial studies using IR spectroscopy played perhaps the most important role in establishing that lipids are characterized by
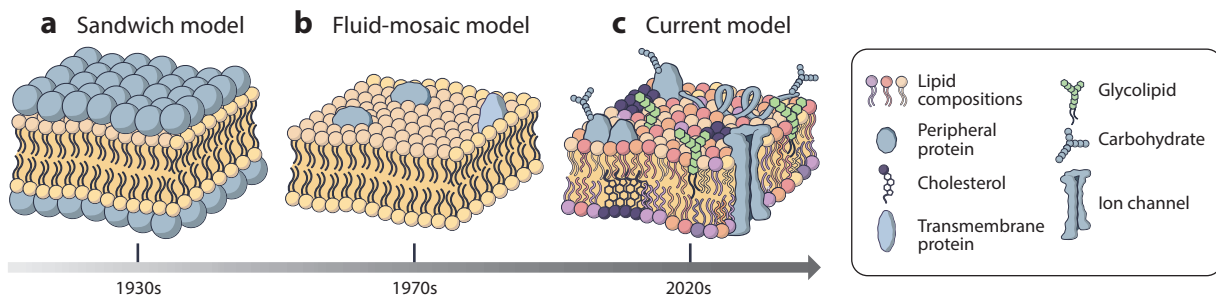
Figure 1
Development of lipid models from the 1930s to the 2020s, showing (*a*) the Davson-Danielli protein sandwich model (9), (*b*) the Singer & Nicolson (13) fluid-mosaic model, and (*c*) the current view of cell membranes. Individual components are indicated in the legend.

liquid-like environments, despite having solid-like properties at the macroscopic scale (15, 16). These measurements informed the fluid character of the supporting lipids in the fluid-mosaic model, suggesting a dynamic bilayer environment.

Nanometer-scale order, compartmentalization, and heterogeneity make lipid membranes significantly richer in complexity compared to previous models (**Figure 1***c*). Modern models incorporate compositions containing a huge diversity of components, as observed in modern lipidomic analyses (17–19). One key aspect of modern lipid membrane models is the presence of compartmentalized domains with distinct lipid and protein compositions, referred to as lipid rafts, which have been observed in artificial and biological membranes. There are clear implications to biological functions that result from colocalizing proteins, as well as modulating the local environment around certain proteins (20–22). Rafts have remained a topic of discussion for over a decade, and this stems mainly from the difficulty in experimentally characterizing their nanometer-scale structure and composition with current techniques. In addition, the concept of rafts rests on the idea of stable domains enriched in certain lipids. Experiments and simulations currently support a more nuanced picture than the lipid raft model, suggesting the formation of dynamic multicomponent local environments that result in transient interactions with specific lipid species, termed the functional paralipidome (22). While transient changes in the local membrane composition can influence the protein conformational landscape, the molecular mechanisms connecting environments with protein modulation are not understood. While techniques such as cryo-electron microscopy have revolutionized the field of membrane structural biology, measuring lipid heterogeneity remains extremely difficult due to a lack of techniques that provide species-specific local environments. Beyond structural measures, there is virtually no time-resolved measurement that can serve to understand the coupling between protein and lipid dynamics across timescales (23, 24).

Lipid raft: dynamic regions in biological membranes enriched in certain components and influencing membrane organization and protein localization

Functional paralipidome: a general model or framework for describing the mutual regulation between membrane proteins and their surrounding lipid microenvironments

Hydrogen bond: a directed electrostatic interaction between polar atoms, involving a protic hydrogen

1.2. What Is Missing from the Current Picture?

While current membrane models include detailed descriptions, one fundamental aspect that remains underexplored is the physical chemistry of membranes with biological compositions, which typically contain hundreds to thousands of lipid species when one considers the diversity in headgroups and acyl chain structures. Why so many lipids? This question largely remains unresolved since biochemical approaches to addressing it have mainly provided indirect information, and the complex interplay between local lipid composition and membrane protein topology as well as colocalization can be particularly complex (25, 26). The fundamental interactions are well understood: headgroup dipole-dipole interactions, hydrogen bonding between headgroups and with interfacial water, tail packing, and steric effects. Recent techniques and experiments, described below, have begun to shed light on the interplay between acyl chain composition and general trends in membrane protein topologies, but fundamental questions remain unaddressed. Specific questions include how the balance of forces between lipid-lipid, lipid-protein, and lipid-water interactions, together with packing, dictates the local membrane environment in membranes containing thousands of lipids. **Figure 2** presents a schematic representation of diverse lipid structures to supplement the current cell membrane model and to emphasize the different charges of functional groups as well as the presence of multiple hydrogen bond donors and acceptors. In brief, this depiction stresses the complex hydrogen-bonding interactions present in multicomponent membranes. The main challenges to achieving a molecular-level understanding stem largely from the lack of well-controlled model systems that incorporate lipid diversity and a range of local interactions, which can be combined with the dearth of experimental techniques to probe species-specific interactions, molecular conformations, and local environments in multicomponent bilayers.
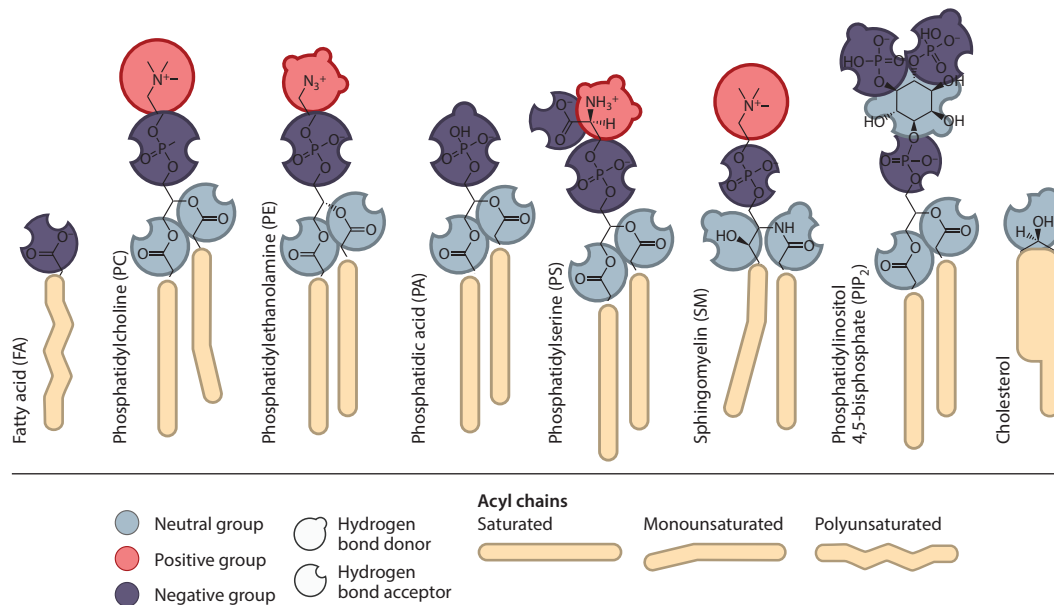
Figure 2

Illustrated structures of common lipids in eukaryotic cells. The structures highlight the complexity in the headgroup structures in terms of charges as well as the number of hydrogen bond donor and acceptor groups. The hydrophobic acyl chains are depicted in yellow, and the headgroup moieties are represented by colors and shapes based on the charge and their ability to donate and accept hydrogen bonds.

1.3. What Is the Outlook?

Developing quantitative models of intermolecular interactions within membrane components is crucial for establishing a general set of mechanistic principles that govern the coupling between environments and protein functions. Key questions that need to be addressed involve the balance of forces stabilizing local lipidic environments around transmembrane proteins, the role of lipid interactions in determining protein structure and stability, and the direct implications for protein function regulation. Formulating hypotheses for these questions remains challenging due to insufficient molecular information and the complexity of intermolecular interactions, such as lipid-protein interactions, lipid-lipid colocalization, and hydrogen bonds among water, lipids, and proteins. The complexity is further compounded by multiple binding sites within lipid headgroups functioning as hydrogen bond donors or acceptors (**Figure 2**). Advancing beyond oversimplified membrane models requires new experimental approaches. Time-resolved and high-sensitivity vibrational spectroscopic methods discussed in this review show potential for providing molecular-level insights into these issues, revealing critical details about the structural and dynamic aspects of the interactions. In particular, the combination of time-resolved vibrational spectroscopy and molecular dynamics (MD) simulations is perfectly suited for investigating structure and dynamics at the interface over a range of timescales from picoseconds to milliseconds. These new approaches can help us arrive at a comprehensive, molecular-level understanding of the interface, uncovering the impacts of the interplay between lipid environments and proteins on associated functionality and biological processes. In the remainder of this review, we summarize the recent developments in ultrafast spectroscopies of model membranes, discuss the strengths and weaknesses of each approach, and provide some specific examples from recent research.

2. VIBRATIONAL SPECTROSCOPY AS A PROBE OF MEMBRANE STRUCTURE AND HETEROGENEITY

Vibrational spectroscopy is a powerful technique to measure conformational ensembles and local environments in complex membranes as vibrational frequencies are highly sensitive to molecular structure, molecular interactions, and local environments. The main challenge in using vibrational spectroscopy lies in the interpretation of spectra within heterogeneous biological mixtures, as overlapping peaks produce ultracongested lineshapes that obscure many features. As a result, at present, model bilayers such as small unilamellar vesicles, which topologically resemble the most fundamental structures of cell membranes, are commonly used as model systems for membrane spectroscopy (27–29). Lipid molecules contain several intrinsic vibrational probes that report on the interfacial interactions and other local environments (**Figure 3**). The O–H stretch of water is a useful vibrational probe given its ability to probe the extended hydrogen bond networks in water (30–32). Furthermore, both the phospholipid headgroups and alkyls can serve as sensitive vibrational probes reporting on specific regions of the bilayer. For example, the phosphate P–O stretching modes are useful for investigating the headgroup hydration, orientations, and lipid-lipid interactions (33–35). Interpreting vibrational lineshapes for phosphate groups can be challenging since the region is congested by the partial overlap among symmetric PO_2^-, asymmetric PO_2^-, and R–O–P–O–R′ stretching modes. Additionally, the ester carbonyls are excellent reporters with well-known characteristics for interfacial hydration, interfacial dynamics, and lipid-protein interactions (27, 28, 35–37). The amide groups of proteins are also strong IR probes for protein structure and local environments (36, 38, 39). Given the rich molecular information derived from vibrational spectroscopy, many IR-based techniques (including time-resolved methods) have been used to investigate membranes and membrane proteins.

Vibrational probe: a functional group with a well-defined vibrational frequency response that can be used to measure local environments and dynamics

2.1. Membrane Structure Characterized by Infrared Spectroscopy

IR techniques, such as Fourier-transform infrared spectroscopy (FTIR), can be used to measure the lineshapes associated with the different vibrational modes in the samples. **Figure 3b** shows an annotated example of an FTIR spectrum with the vibrational modes from a phospholipid headgroup, ester linkage, acyl chain, and water molecule across a broad spectral range from 1,000 to 4,000 cm^{-1}. The center frequencies and lineshapes of vibrational modes in IR spectra provide molecular information about the phase of the membrane as described by the ordering of the acyl chains, interfacial hydrogen bond networks of water reported by the –OH vibrational mode, and lipid hydration by phosphate headgroup and ester linkage (40–42).

The ester carbonyl–stretching mode spans a region between 1,725 and 1,740 cm^{-1} depending on the lipid conformation and interfacial hydration level. In solution, the IR lineshape of lipid ester carbonyl is broad and asymmetric due to the presence of two hydrogen-bonding species: carbonyls with no hydrogen bond and carbonyls with a single hydrogen bond. Abundant lipid species such as phosphatidylcholine (PC) do not contain hydrogen bond donors, and thus, any hydrogen bonds are with interfacial water molecules. Deconvolving the measured lineshape using peak models can quantify the hydrogen bond populations at the water-lipid interface, thereby providing insights into water penetration into the interfacial region, carbonyl orientations, and interactions with the aqueous environment. As an example, an FTIR spectrum of 1-palmitoyl-2-oleoyl-*sn*-glycero-3-phospho-L-serine (POPS) and 1,2-dimyristoyl-*sn*-glycero-3-phosphocholine (DMPC) at a 1:9 molar ratio is shown in **Figure 4**. The ester carbonyl–stretching region exhibits an asymmetric IR lineshape described by two overlapping peaks corresponding to two distinct hydrogen bonded carbonyl species: zero hydrogen bond (0HB) and one hydrogen bond (1HB). The 1HB peak position is red-shifted by approximately 15 cm^{-1} from the 0HB peak position as a result of the induced electric field by the partial positive charge on the hydrogen atom (43). Fitting
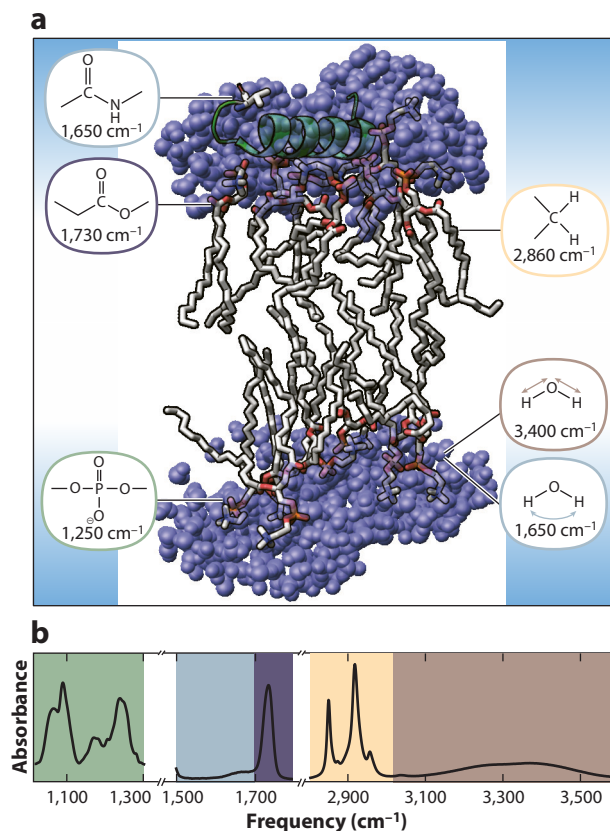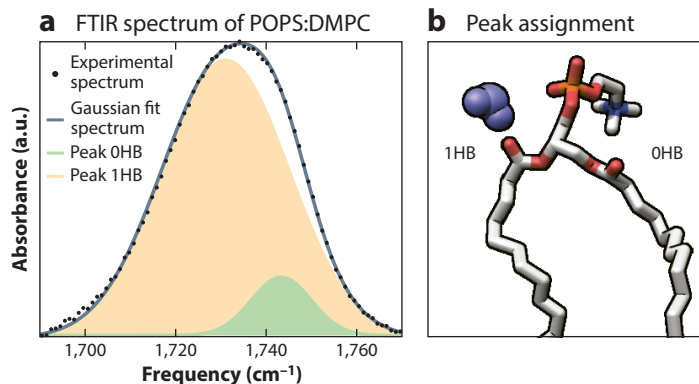
Figure 3

Illustration of common vibrational probes in lipid membranes. (*a*) A lipid bilayer section with a bound helical peptide (*green*) showing the different vibrational probes. Carbon, oxygen, nitrogen, and phosphate atoms are colored as gray, red, blue, and orange, respectively. Interfacial water molecules are shown in translucent blue. The approximate frequency of each probe is provided below the corresponding chemical structure.
(*b*) Fourier-transform infrared spectroscopy spectrum of a dried 1,2-dimyristoyl-*sn*-glycero-3-phosphocholine (DMPC) lipid film measured under ambient conditions. The shaded areas indicate the frequency regions of the phosphate stretching mode (*green*), –OH bending mode (*blue*), amide I stretching mode (*blue*), ester carbonyl stretching mode (*purple*), –CH$_2$– stretching mode (*yellow*), and –OH stretching mode (*brown*). The horizontal axis shows the frequency in wavenumbers, and the vertical axis represents the infrared absorbance in arbitrary units. The absorbances across different regions are scaled for clarity.

the FTIR spectrum with two Gaussian profiles can help quantify the 0HB and 1HB populations, which involves computing the peak areas from the Gaussian fittings and determining the relative extinction coefficients of the two hydrogen-bonding species (44). Interfacial water plays a pivotal role in cell integrity and functionality. The hydrogen bond population at the lipid-water interface is affected by the formation of lipid domains/microdomains and protein binding. The control over cellular processes exerted by lipid membranes may also, in part, derive from the distinct hydration properties of the membrane interface. Therefore, exploring hydrogen bond populations serves as both an indirect measure of the spatial organization within lipid bilayers, modulated by membrane compartmentalization and protein binding, and a direct indicator of the hydration characteristics at the membrane interface. This quantity can also be compared with MD simulations, allowing for a direct and one-to-one connection between experiments and simulations.

a FTIR spectrum of POPS:DMPC

b Peak assignment

Figure 4

Example of Fourier-transform infrared spectroscopy (FTIR) spectrum for 1-palmitoyl-2-oleoyl-*sn*-glycero-3-phospho-L-serine (POPS):1,2-dimyristoyl-*sn*-glycero-3-phosphocholine (DMPC) vesicles at a 1:9 ratio in 3-(*N*-morpholino)propanesulfonic acid (MOPS) buffer in D_2O, with an illustration of two hydrogen-bonding species in a lipid. (*Left*) Spectrum fitted with two Gaussian profiles [one hydrogen bond (1HB) in *yellow* and zero hydrogen bond (0HB) in *green*]. Dotted and solid lines show the experimental spectrum and the Gaussian fit spectrum, respectively. (*Right*) Illustration of a phosphatidylcholine lipid with one carbonyl hydrogen bonded to a water molecule (1HB) shown as slate blue spheres, and the other without a hydrogen bond. Hydrogen atoms in the lipid are omitted for clarity. Carbon, oxygen, nitrogen, and phosphate atoms are colored as gray, red, blue, and orange, respectively.

Measuring spectra with well-defined compositions, including those lipids shown in **Figure 2**, enables researchers to examine each component's influence on the interfacial properties of model systems. Furthermore, temperature-dependent FTIR spectra are useful for investigating lipid phase transitions and determining enthalpies and entropies associated with hydrogen bond formation (45). In addition to the ester carbonyl stretch, other vibrational modes also provide information about interfacial environments, morphologies, and local interactions. For example, a redshift in $-CH_2-$ stretching peaks indicates more ordered acyl chains, as, for example, in the gel phase (46). Thus, this spectral region can be used to track phase transitions in model bilayers. It is important to note that probing intrinsic vibrational modes yields an ensemble-averaged view across oscillators. For instance, the hydrogen bond number obtained from the FTIR spectrum of POPS:DMPC represents the average number for all ester groups in both lipid species, and hydrogen bonds formed specifically with POPS cannot be differentiated from those with DMPC. Consequently, if an altered composition in lipid vesicles has a low concentration or weak signal, discerning the changes in lineshapes solely based on linear IR spectra becomes challenging. Isotope labeling is a good approach to isolate the contributions from different lipid compositions and investigate the effects of individual components. For instance, the ester carbonyl groups of PC can be isotope edited by ^{13}C, which gives rise to a red-shifted carbonyl stretch 40 cm^{-1} away from the carbonyl stretch of unlabeled phosphatidylserine (PS) (47). As a result, the effects of PC or PS can be studied separately, though the method is limited to investigating species with relatively high concentrations.

2.2. Transient Interactions in Lipid Membranes

Static spectra offer ensemble-averaged structural views of equilibrium conformations. Obtaining a more complete view of membranes requires measuring local environments and interactions, specifically molecular motions on sub-picosecond timescales. These measurements require

ultrafast time-resolved spectroscopies such as two-dimensional infrared (2D IR) spectroscopy and two-dimensional sum-frequency generation (2D SFG) spectroscopy, which have become valuable tools for detecting and characterizing dynamic processes in biological systems due to their ability to combine molecular information with high time resolution. For example, the lipid-water interface, a crucial local environment, is frequently studied at various temporal resolutions relevant to the dynamics of hydrogen bond fluctuation and reorganization. Water dynamics can correlate with changes in membrane bilayer structure during processes like cell fusion, protein insertion, and protein folding. As a result, the polarity, stability, and fluidity of the cell membrane interface can be inferred through the investigation of hydration dynamics using 2D IR and 2D SFG spectroscopies.

2.2.1. Structure and dynamics by two-dimensional infrared spectroscopy.

2D IR spectroscopy is popular for studying complex molecular systems—such as biomolecules, polymers, and materials—to elucidate their structure, dynamics, and interactions. 2D IR spectroscopy uses three ultrafast pulses, two pump pulses, and one probe pulse, each with a temporal width of approximately 100 fs. The absorbance in 2D IR spectroscopy is correlated with the peak intensity of three laser pulses, thus improving its capability in detecting weak signals and discerning small changes in the IR lineshape. In 2D IR spectra (**Figure 5a**), the horizontal and vertical axes represent the pump and probe frequencies, respectively. The positive peaks correspond to the transition between ground and first excited states, known as the ground state bleach (GSB). The negative peaks denote the vibrational transition between the first and second excited states, namely the excited state absorption (ESA). The frequency of ESA is downshifted from the GSB due to the anharmonicity of the oscillation. The spectral widths of contoured peaks along the diagonal and antidiagonal of 2D IR spectra report on the inhomogeneous and homogeneous broadening mechanisms. Overall, the 2D lineshapes report on the distribution of local environments and their fluctuations (48, 49).

Dynamics of local environments surrounding the IR probes can be detected on a sub-picosecond timescale by varying the delay between pump and probe pulses (t_2). In 2D IR spectra,
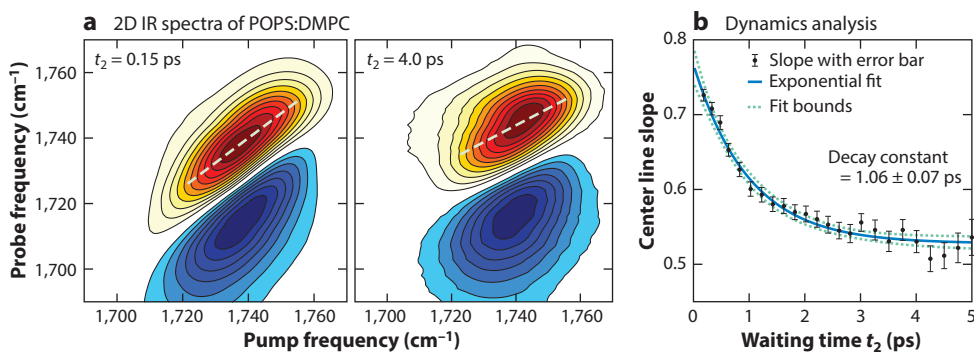
Figure 5

Example of two-dimensional infrared (2D IR) spectra and dynamics analysis for 1-palmitoyl-2-oleoyl-*sn*-glycero-3-phospho-L-serine (POPS):1,2-dimyristoyl-*sn*-glycero-3-phosphocholine (DMPC) vesicles at a 1:9 molar ratio in 3-(*N*-morpholino)propanesulfonic acid (MOPS) buffer in D_2O. (*a*) 2D IR spectra at selected waiting times of 0.15 ps and 4.0 ps. The positive peaks (*red contours*) represent the transition between the ground and first excited states, and the negative peaks (*blue contours*) represent the transition between the first and second excited states. The solid black line represents the diagonal where pump and probe frequencies are equal. The dotted light gray line spanning the ridge of the maximum intensity indicates the center lines. (*b*) Dynamics analysis of time-dependent 2D IR spectra by the center line slope method. The slopes versus the waiting time t_2 are fitted with a single exponential decay, where the decay constant from fitting is 1.06 ± 0.07 ps.

peaks are elongated along the diagonal at early waiting times and become rounder at later waiting times as pump and probe frequencies gradually decorrelate due to the frequency fluctuations when ensembles initially excited at a given frequency become randomized. This process is referred to as spectral diffusion. In essence, waiting-time-dependent 2D IR spectra measure the frequency-frequency correlation function (FFCF) of each vibrational probe within the system (48, 50, 51). The frequency decorrelation times, encoded within the 2D lineshapes, can be extracted using numerical analysis methods such as the center line slope (CLS) (52), nodal line slope (53, 54), ellipticity parameter (55), or fitting to a model response function (56, 57).

Compared to FTIR spectra, 2D IR spectra spread the information onto two frequency axes, which not only capture additional structural information through the 2D lineshapes and cross-peak intensities but also access local environments around vibrational probes by the evolution of the lineshapes as a function of the pump-probe delay (36, 58, 59). In addition, while FTIR spectra require measuring a separate background of the buffer solution for subtraction, 2D IR spectra are often measured without a separate background. This is because, in water, the low oscillator strengths of the solvent vibrations and broad lineshapes naturally suppress the background, thus removing the necessity of background subtraction. Furthermore, given the narrow lineshapes in 2D IR spectra, small differences that can be difficult to observe in FTIR spectra are often easier to analyze in the corresponding 2D IR spectra; as such, it is often useful to extract a corresponding 1D spectrum from a 2D IR spectrum (60, 61). A recent, robust method for extracting the IR lineshape is pump slice amplitude (PSA) analysis, which calculates the difference between the maxima and minima across a series of pump-axis slices through the 2D IR spectrum (62). The PSA method produces lineshapes comparable to FTIR spectra of the same system but with the advantages of eliminating artifacts due to anharmonicity and suppressing the background.

Examples of 2D IR spectra and lineshape analysis for POPS:DMPC at a 1:9 molar ratio are depicted in **Figure 5**. **Figure 5*a*** displays the 2D IR spectra in the ester carbonyl region at early (0.15 ps) and late (4.0 ps) waiting times. The signal is centered at approximately 1,740 cm^{-1}, consistent with the FTIR spectrum (**Figure 4**). The broad band along the diagonal originates from the two hydrogen-bonding species (0HB and 1HB), as described previously (**Figure 4**), with 1HB red-shifted by approximately 15 cm^{-1}. The evolution of the lineshapes as a function of the waiting time (t_2) is used to extract the dynamics of the local environments around lipid ester carbonyl groups. In **Figure 5**, we provide an example of 2D lineshape analysis using the CLS method (63). In brief, the CLS is the slope of the line connecting the maxima of peaks, which are a series of cuts through the 2D spectrum parallel to the pump frequency axis. CLS decays indicate the loss of frequency correlation. In **Figure 5*b***, the CLS for a lipid vesicle sample is calculated and plotted versus waiting time up to 5 ps. Since the CLS decay measures the FFCF decay [$C(t_2)$], it can be represented by the following equation using the standard Bloch model (48):

$$C(t_2) = \langle \delta\omega(t_2)\,\delta\omega(0) \rangle = \frac{\delta(t_2)}{T_2} + \Delta^2 e^{-\frac{t_2}{\tau_1}} + \Delta_0^2,$$

where $\delta\omega(t)$, Δ^2, τ_1, and Δ_0^2 are the frequency fluctuation at time t, amplitude of frequency fluctuations, decay constant, and static inhomogeneity components, respectively. T_2 is the constant giving rise to the homogeneous width, and t_2 is the waiting time between pump and probe pulses. The FFCF decay constant for the ester carbonyl stretch is determined to be approximately 1.07 ps for the 1:9 POPS:DMPC vesicles.

In membranes, the interfacial hydrogen bond network is disrupted due to interactions with the lipid headgroups and an imbalance of donors and acceptors. In bulk water, the hydrogen bond dynamics are as fast as hundreds of femtoseconds (32, 64), but the dynamics become slower at the interface (a few picoseconds). In general, disordered water networks exhibit slower reorganization

Frequency-frequency correlation function (FFCF): a measure of the evolution of the local environment as reported by the frequency fluctuations around a vibrational probe

Pump slice amplitude (PSA) analysis: an analysis method to extract Fourier-transform infrared spectroscopy–like lineshapes from two-dimensional infrared spectra

dynamics because the hydrogen bond switching process is a concerted process involving multiple water molecules (36, 64). However, since the spectrum measures frequency fluctuations, not only hydrogen bond switching but also local fluctuations in hydrogen bond distances and angles significantly contribute to the measured loss in frequency correlation (29, 65). Measured dynamics from 2D IR spectroscopy can indicate the changes of water networks at the lipid-water interface and hence the effects of variables such as the membrane composition, crowding, or interfacial localization of ions.

Here, we show an example of how ester carbonyl 2D IR spectra provide direct access to the environment and dynamics at the lipid-water interface. It is important to emphasize that while 2D IR spectroscopy is not a surface-specific technique, the vibrational reporters are located precisely at the ~1-nm interface between the hydrophobic acyl chain region and bulk-like water beyond the headgroup region, and thus the measurements provide interfacial information. There are multiple avenues for applying 2D IR spectroscopy to understand how headgroup composition and lipid-lipid interactions determine the interfacial environments, contributing to a more complete understanding of membranes, ranging from the effects of headgroup charges (57) or ion localization (66) to the effects of transmembrane crowding on interfacial water networks (67).

2.2.2. Interfacial environment by sum-frequency generation spectroscopy.
The membrane interaction with its environment is crucial for membrane function and stability. 2D IR spectroscopy can detect the local environment of the lipid interface by probing the frequency fluctuations of lipid ester carbonyl groups, where the lineshape and dynamics of 2D IR spectra are correlated with the water network at the interface. However, direct detection of the interfacial environment around the cell membrane can be difficult to perform with 2D IR as the bulk water dominates the final signal and it is not possible to measure the interface-specific signals. Thus, a technique with interface selectivity is essential for isolating interfacial water molecules and measuring specific interactions involving water at the membrane interface.

Sum-frequency generation (SFG) spectroscopy is frequently used for studying interfaces and surfaces, providing insights into molecular interactions and structures at these critical boundaries. 1D SFG, developed in the last 30 years, provides access to ensemble-averaged local environments at the interface, including the dipole orientation, and specific hydrogen bond networks, though heterodyne detection needs to be incorporated to obtain an unambiguous measure of the vibrational response (68). The SFG method uses a narrowband visible pulse combined with a broadband IR pulse, which generates an output signal at the sum frequency of two input pulses if vibrational probes in the system are resonant with the IR pulse. The output SFG pulse is mixed with a local oscillator to deconvolve the phase information. 2D SFG spectroscopy, which incorporates additional pulses to resolve dynamics, has advanced significantly over the past 5 years, becoming a powerful tool to investigate interfacial dynamics of membranes (69). An IR pump pulse is implemented in SFG to provide a frequency-resolved excitation axis, similar to the pump axis in 2D IR spectroscopy. 2D SFG can be interpreted as a frequency-resolved IR pump and SFG probe technique. 2D SFG has the advantage of high selectivity towards interfacial regions with anisotropic molecular orientations, inherent to second-order nonlinear optical processes (70). To avoid the interference of multiple interfaces, a monolayer at the air-water interface is usually prepared (**Figure 6**) (36, 71). Using 2D SFG, the dynamics of the hydrogen bonded and free -OH stretches of water are probed through characteristic peaks in the region of 3,200 to 3,700 cm^{-1}, providing direct access to the hydrogen bond networks of water within the first few solvation shells around the lipid headgroups.

2D SFG has been recently used to measure interfacial water dynamics for the negatively charged lipid 1,2-dipalmitoyl-*sn*-glycero-3-phosphoglycerol (DPPG) versus the positively
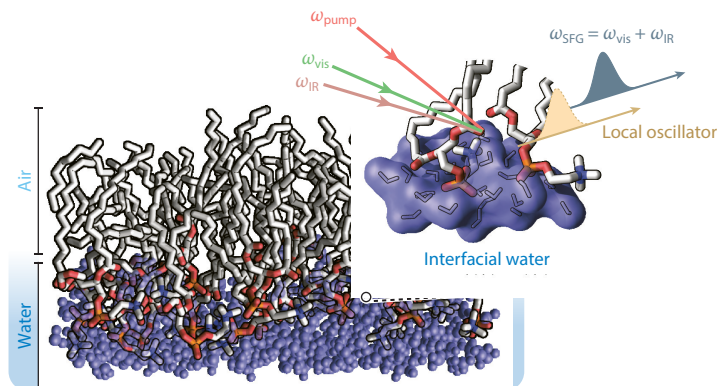
Figure 6

Diagram of a two-dimensional sum-frequency generation (2D SFG) configuration for measuring interfacial water molecules with a lipid monolayer at the air-water interface. A pump beam (*red*) is introduced to resolve the excitation frequency. The other two input beams, green for visible (vis) light and pink for infrared (IR), act as the probe. The output signal (*gray blue*) is generated at the sum frequency of visible and IR wavelengths. A local oscillator (*tan*) is introduced for heterodyned detection to resolve phase information.

charged surfactant 1,2-dipalmitoyl-3-trimethylammonium-propane (DPTAP) (72). The lipid monolayers are prepared on isotopically diluted water, where the –OH stretch of HOD gives rise to the majority of the SFG signal in the –OH stretching region. Interestingly, steady-state SFG spectra of DPPG and DPTAP show opposite signs (**Figure 7*a,b***), indicating the opposite net orientation of interfacial water due to the negatively and positively charged lipid headgroups. However, the peak position and lineshape in the SFG spectra are similar for DPPG and DPTAP, demonstrating the similar hydrogen bond environment, despite the opposite charges.

In addition, 2D SFG spectroscopy probes the picosecond spectral diffusion of the –OH stretch (**Figure 7*c,d***). The interpretation of the lineshapes is similar to that of 2D IR spectra, where the evolution of the lineshapes provides a measure of the FFCF of the interfacial water molecules. The time-dependent 2D SFG spectra are analyzed by the CLS method, where different dynamics are observed for DPPG and DPTAP. In brief, the negatively charged lipid layer disrupts the water network and suppresses the fast hydrogen-bonding dynamics due to strong hydrogen bonds involving the hydrophilic DPPG phosphatidylglycerol headgroup (**Figure 7**). In contrast, the positively charged DPTAP layer does not have significant effects on the interfacial water ordering and dynamics, as evidenced by the fast dynamics that are comparable to bulk water (32, 64). In summary, 2D SFG directly probes interfacial environments, providing a specific view of the relation between membrane composition and water dynamics. The technique can also be used to study membrane proteins (73, 74), pH effects (75), and cation effects (76) in the context of lipid membranes.

2.3. Surface-Enhanced Infrared Absorption Spectroscopy

Surface-enhanced infrared absorption spectroscopy (SEIRAS) is frequently used for investigating molecular structure and reactions at metal surfaces, offering valuable information about surface chemistry and catalytic processes. It has emerged as a useful technique for studying lipid membranes, as it significantly enhances detection sensitivity for monitoring conformation and structure at single-bilayer interfaces without interference from bulk solvent backgrounds. In SEIRAS, a thin, nanoscale-roughened, metal film is deposited on an attenuated total reflectance

Surface-enhanced infrared absorption spectroscopy (SEIRAS): an approach to measure surface-sensitive vibrational spectra with a penetration depth of ∼100 nm using gold nanoparticles
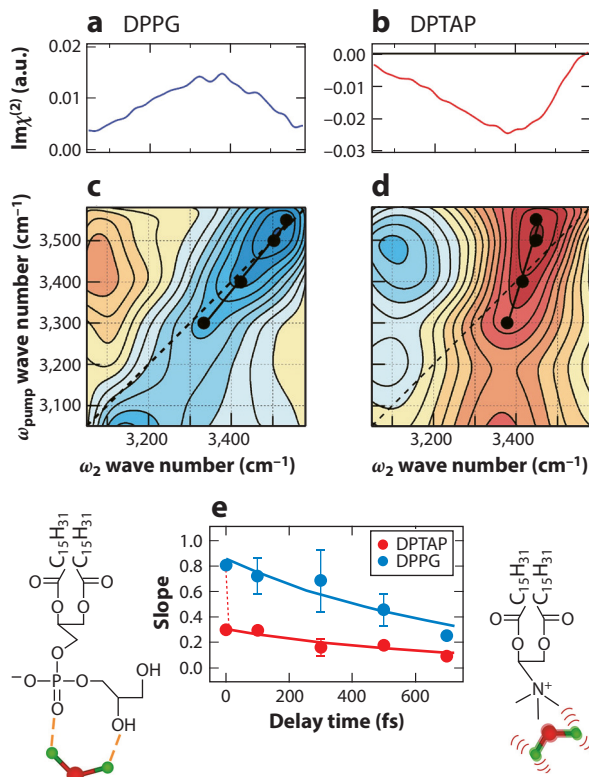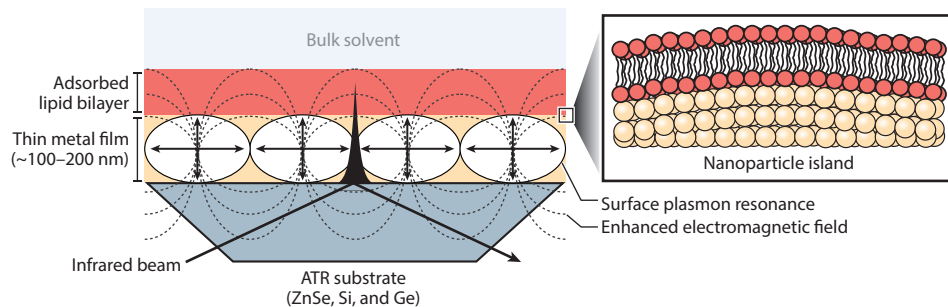
Figure 7

Heterodyne-detected sum-frequency generation (SFG) and two-dimensional sum-frequency generation (2D SFG) spectra of water at the air-water interface of positively and negatively charged lipids. (*a,c*) Steady-state and 2D SFG spectra at the 1,2-dipalmitoyl-*sn*-glycero-3-phosphoglycerol (DPPG) interface. (*b,d*) Steady-state and 2D SFG spectra at the 1,2-dipalmitoyl-3-trimethylammonium-propane (DPTAP) interface. The horizontal and vertical axes represent the ω_2 (SFG probe) and ω_{pump} [infrared (IR) pump] frequencies, respectively. (*e*) Center line slopes for DPPG (*blue*) and DPTAP (*red*) interfaces as a function of the IR to SFG delay. Schematic models for DPPG (*left*) and DPTAP (*right*) interfaces are also shown at the bottom. Figure adapted with permission from Reference 68; copyright 2017 American Chemical Society.

(ATR) crystal, enabling the IR beam to excite local surface plasmons in the metal. The plasmonic near-field enhancement partially penetrates ~100 nm from the surface into the sample (**Figure 8**). The IR signal is greatly enhanced for molecules adsorbed on the metal surface, with surface plasmon polariton modulation resulting in a 10–100× increase in IR absorption (77). Specifically engineered nanostructured materials can provide even higher enhancement factors (78–81).

Initial developments provided a 20× enhancement in the IR absorption of organic monolayers on thin metal films. Osawa and coworkers (82–84) later noted general properties and the theory for SEIRAS: The IR enhancement is general for nonvolatile molecules; the enhancement increases for molecules strongly chemisorbed on the metal film; and the effect is observed only for the first few adsorbed monolayers. More recent models provide a surface-average enhancement factor and IR penetration depth from experiment as the ratio of molar absorptivities of SEIRAS to the bulk (85).

A general experimental procedure for SEIRAS involves the formation of a metal layer, typically 100–200 nm of gold or silver, on a polished ATR substrate through electrochemical deposition (86, 87), metal vapor deposition in vacuum (88–92), or electroless (chemical) deposition (93, 94).

Bulk solvent

Adsorbed lipid bilayer

Thin metal film (~100–200 nm)

Infrared beam

ATR substrate (ZnSe, Si, and Ge)

Nanoparticle island

Surface plasmon resonance
Enhanced electromagnetic field

Figure 8

Illustration of an experimental setup of surface-enhanced infrared absorption spectroscopy with an adsorbed lipid bilayer (*red*) on a metal surface (*tan*). The blue trapezoid represents the attenuated total reflectance (ATR) prism. The dashed lines represent the enhancement in the electromagnetic field from the generated surface plasmon resonances. The box on the right shows a zoomed-in view of the lipid-metal interface. Figure adapted with permission from Reference 77; copyright 2010 Wiley-VCH.

The latter technique yields more stable metal films and larger islands on the surface. The enhancement factor depends on the thickness of the film, as thicker films exhibit increased IR reflectivity. Because of the rapid decay in the enhancement penetration depth, the solvent absorption is minimized. This allows for direct study of specific regions in the membrane with the resolved intrinsic vibrational probes in the lipid membrane. SEIRAS is useful for studying interfacial properties, such as water structure near a supported lipid bilayer (95–97), with very low penetration depth into the bulk. Lipid membranes have large potentials because of concentration or pH gradients, and SEIRAS enables the study of the effects of fields and potentials in biological systems using vibrational probes to measure the local electrostatic environments. Additionally, SEIRAS provides the ability to rapidly change sample conditions such as pH or ion concentrations and the ability to measure kinetics on the timescale of seconds to hours (98).

In typical SEIRAS measurements, a lipid vesicle solution is prepared and deposited on the metal surface. A spacer of adsorbed molecules can be used to form floating lipid bilayers (96, 97), mitigating any effects from the metal surface on the membrane properties. The vesicles rupture and self-assemble as an ordered monolayer on the surface, eventually forming a bilayer (99, 100). The bulk solvent can be easily replaced with different solvents, and solutions containing transmembrane proteins can also be added to study protein insertion (101) (**Figure 9**) or potential-dependent structural changes (102). SEIRAS can also be used to monitor time-resolved in situ processes, such as the expression and folding/inserting of transmembrane proteins into lipid membranes (98). The folding/insertion process and conformational changes can be tracked by the lineshape of amide bands over time.

Relevant advancements in SEIRAS techniques include time-resolved SEIRAS (103, 104), surface-enhanced ultrafast IR spectroscopy (105), and surface-enhanced 2D IR (SE2DIR) spectroscopy (102, 106–109). SE2DIR spectroscopy enables the measurement of species with low molar absorptivity in both transmission and reflection geometries with deposited metals <10 nm thick (105, 106). A new plasmonic design has been reported to maximize surface coverage and enhancement while reducing background signals and lineshape distortions (107). The capabilities and recent developments of SEIRAS techniques demonstrate that this method is suited to address key questions surrounding lipid membranes. The low penetration depth into the sample allows one to study the membrane structure, morphology, interface, and local membrane environments with enhanced single-bilayer detection sensitivity while minimizing signal contributions
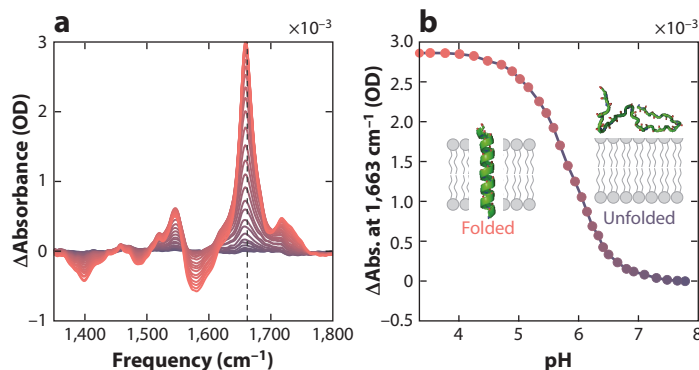
Figure 9

Surface-enhanced infrared absorption spectroscopy spectra of the titration of a pH-low insertion peptide (pHLIP) inserting/folding into a 1-palmitoyl-2-oleoyl-glycero-3-phosphocholine (POPC) bilayer. (*a*) Amide I absorbance increases as pH decreases (*purple* to *red*). (*b*) The change in absorbance at 1,663 cm^{-1} is plotted as a function of pH. The inset illustrations show pHLIP in an inserted/folded state in the membrane at low pH compared to high pH.

from the bulk solvent. The ability to resolve signals of protein amide bands allows one to elucidate the effect of lipid-protein interactions on protein conformation and the mechanism and kinetics of the folding/inserting of transmembrane proteins. For example, one can envision differential measurements using isotope-labeled lipids in multicomponent bilayers to examine the functional paralipidome with model peptides. Other variables such as pH, the peptide composition, or ion concentrations can be easily altered by replacing the solvent after lipid bilayers are formed on the SEIRAS substrate. Time-resolved and ultrafast SEIRAS, similar to 2D IR spectroscopy, can measure kinetics on the picosecond timescale, and SE2DIR spectroscopy further improves the signal-to-noise ratio in measurements. Furthermore, there are other possibilities to investigate intact plasma membranes, for example, by combining SEIRAS with cell-unroofing techniques (110).

3. INTERPRETATION OF EXPERIMENTS THROUGH MOLECULAR DYNAMICS SIMULATIONS

3.1. Molecular Dynamics Simulations

Interpreting spectra is one of the main challenges due to the complex lineshape and spectral congestion in multicomponent systems. For example, when analyzing a mixture, the resulting spectra provide an average of all vibrational modes across different species, making it difficult to separate and identify individual contributions (57, 66, 111). Isotope labeling can be used to isolate individual species provided that the labeled species are present at high concentrations. In addition, interface-specific spectra can be difficult to interpret as coupling and delocalization make vibrational assignments difficult, even for well-defined interfaces such as the air-water interface (68, 112). Evidently, lipid membranes add complexity as the diversity of lipids, proteins, cholesterol, and carbohydrates makes for a highly heterogeneous interfacial environment. For these reasons, molecular insights are most often derived by computing spectra based on atomistic modeling, and MD simulation is an ideal technique to provide molecular ensembles for spectra computation (113–117).

Computed spectra provide the most direct route to interpret spectral features arising from interactions with lipids, water, proteins, ions, and other small molecules. Computing spectra from structural ensembles requires the use of models, such as electrostatic maps, that translate the local

electrostatic environment around each oscillator to a frequency shift (118). The advantage of these maps is that they provide a computationally tractable means of generating spectra for systems that contain hundreds of oscillators due to their computational efficiency (119). These structure-based vibrational models provide a one-to-one comparison between experiment and simulation as well as a route to interpret complex lineshapes in terms of local environments. Simulating short-range dynamics, such as hydrogen bond fluctuations and reorganization, typically requires short trajectories of a few hundred picoseconds. Overall, MD simulations have become increasingly reliable for relatively uniform membranes composed of one to two types of phospholipids, with simulated results now achieving near-quantitative agreement with experiments (111, 120, 121).

3.2. Challenges of All-Atom Simulations

Sampling is one of the ongoing challenges for simulations, which becomes notably more formidable when dealing with complex or heterogeneous membranes containing proteins. Obtaining equilibrated ensembles is difficult because of the large number of degrees of freedom, relative lack of experimental references to dictate initial ensembles, and the slow lipid reorganization timescales (122–124). New algorithms such as Molecular Dynamics with Alchemical Steps (MDAS) have been developed to mitigate the conformational sampling problem (122). The MDAS algorithm combines conventional MD simulations with alchemical trajectories, which swap the positions of randomly selected pairs, analogous to Monte Carlo simulations but using a short trajectory where the parameters of two lipids are exchanged. In addition, within the functional paralipidome model described above, different proteins can recruit distinct lipid environments, including specific subtypes with various headgroups. The local membrane properties can be modulated by external factors to accommodate protein structure and function in membranes (22). Enhanced sampling methods are useful for equilibrating such complex systems.

Another challenge is the parameterization of lipid force fields (124–126). Several all-atom lipid force fields, including CHARMM36, AMBER (LIPID21), Slipids, and polarizable models, have been published and benchmarked in combination with various water models (127–130). However, due to the complex lipid interactions and the number of lipid species, achieving quantitative agreement between simulated and experimental observables beyond simple bilayers remains a challenge (124, 126). Moreover, bilayer properties are sensitive to weak and long-range interactions, which are difficult to accurately parameterize (131–133). Modern computer software and recent multiscale models combined with machine learning present new avenues for further development (125, 134, 135). There are many opportunities to use vibrational techniques for characterizing interactions in heterogeneous samples and for providing useful molecular-level information for benchmarking simulations (43, 121, 136, 137). Using these spectroscopic techniques on a library of lipid compositions and modern MD simulations could be a powerful approach to measure the balance of lipid-lipid, lipid-protein, and lipid-water forces that lead to the heterogeneity in multicomponent membranes.

4. ONGOING CHALLENGES, PROSPECTS, AND OPPORTUNITIES

Vibrational spectroscopy has advanced enormously over the past decade. The spectroscopic approaches discussed above have offered exciting opportunities to investigate membrane structure and dynamics in increasingly complex systems. One key challenge is achieving spatial resolution and the ability to map the nanometer-scale heterogeneity for lipid organization. Nano-IR microscopy, which uses an atomic force microscope tip to localize electric fields and thereby achieve spatial resolution, could be coupled with time-domain techniques to directly probe membrane structure and dynamics from single bonds to the micrometer length scale (138–141).

The second challenge is membrane asymmetry. Specialized lipids are often enriched in microdomains and unevenly distributed across leaflets. For example, PS is mainly distributed in the inner leaflet of the plasma membrane in healthy eukaryotic cells due to the activity of transporter proteins. Therefore, characterizing the PS distribution is crucial for understanding the functions of lipids in cellular homeostasis and membrane trafficking. SFG spectroscopy could provide a direct measure of the net orientation, and thus measure enrichment across the leaflets. However, challenges would certainly arise in future experimental designs of in vivo SFG measurements of plasma membranes.

Another challenge, as discussed above, is the large diversity of lipid species present in cell membranes. While simple lipid compositions have been extensively investigated, building more complex or realistic lipid membranes remains challenging. Vibrational spectroscopy provides ensemble-averaged results across all oscillators, irrespective of lipid species, and isotope labeling, e.g., ^{13}C (41, 47, 142, 143), or functional-group labeling, e.g., nitrile or thiocyanate groups (144, 145), can help identify the contribution of each species individually. MD simulations can also help interpret complex spectra. However, building heterogeneous membranes introduces complicated interactions and requires more sensitive vibrational techniques to probe the subtle yet important effects introduced by minor lipid species. Meanwhile, building synthetic systems with artificial lipids (146, 147), lipid nanodiscs (148), and artificial channels (149) can serve as useful platforms to study lipid-protein interactions in minimalistic or well-defined environments.

DISCLOSURE STATEMENT

The authors are not aware of any affiliations, memberships, funding, or financial holdings that might be perceived as affecting the objectivity of this review.

ACKNOWLEDGMENTS

LITERATURE CITED

1. Spector AA, Yorek MA. 1985. Membrane lipid composition and cellular function. *J. Lipid Res.* 26(9):1015–35

2. Sackmann E, Tanaka M. 2021. Critical role of lipid membranes in polarization and migration of cells: a biophysical view. *Biophys. Rev.* 13(1):123–38

3. Yèagle PL. 1989. Lipid regulation of cell membrane structure and function. *FASEB J.* 3(7):1833–42

4. Lombard J, López-García P, Moreira D. 2012. The early evolution of lipid membranes and the three domains of life. *Nat. Rev. Microbiol.* 10(7):507–15

5. Deamer D. 2017. The role of lipid membranes in life's origin. *Life* 7(1):5

6. Gupta S, Ashkar R. 2021. The dynamic face of lipid membranes. *Soft Matter* 17(29):6910–28

7. Gorter E, Grendel F. 1925. On bimolecular layers of lipoids on the chromocytes of the blood. *J. Exp. Med.* 41(4):439–44

8. Edidin M. 2003. Lipids on the frontier: a century of cell-membrane bilayers. *Nat. Rev. Mol. Cell Biol.* 4:414–18

9. Danielli JF, Davson H. 1935. A contribution to the theory of permeability of thin films. *J. Cell. Comp. Physiol.* 5(4):495–508

10. Bernal JD, Crowfoot D. 1934. X-ray photographs of crystalline pepsin. *Nature* 133:794–95

11. Chapman D. 1965. *The Structure of Lipids by Spectroscopic and X-Ray Techniques*. New York: Wiley

12. Chapman D, Williams RM, Ladbrooke BD. 1967. Physical studies of phospholipids. VI. Thermotropic and lyotropic mesomorphism of some 1,2-diacyl-phosphatidylcholines (lecithins). *Chem. Phys. Lipids.* 1(5):445–75

13. Singer SJ, Nicolson GL. 1972. The fluid mosaic model of the structure of cell membranes. *Science* 175(4023):720–31

14. Nicolson GL. 2014. The fluid-mosaic model of membrane structure: still relevant to understanding the structure, function and dynamics of biological membranes after more than 40 years. *Biochim. Biophys. Acta* 1838(6):1451–66

15. Chapman D. 1975. Phase transitions and fluidity characteristics of lipids and cell membranes. *Q. Rev. Biophys.* 8(2):185–235

16. Chapman D. 1966. Liquid crystals and cell membranes. *Ann. N.Y. Acad. Sci.* 137(2):745–54

17. Brügger B. 2014. Lipidomics: analysis of the lipid composition of cells and subcellular organelles by electrospray ionization mass spectrometry. *Annu. Rev. Biochem.* 83:79–98

18. Quehenberger O, Armando AM, Brown AH, Milne SB, Myers DS, et al. 2010. Lipidomics reveals a remarkable diversity of lipids in human plasma. *J. Lipid Res.* 51(11):3299–305

19. Yang K, Han X. 2016. Lipidomics: techniques, applications, and outcomes related to biomedical sciences. *Trends Biochem. Sci.* 41(11):954–69

20. Levental I, Levental KR, Heberle FA. 2020. Lipid rafts: controversies resolved, mysteries remain. *Trends Cell Biol.* 30(5):341–53

21. Levental I, Veatch SL. 2016. The continuing mystery of lipid rafts. *J. Mol. Biol.* 428(24):4749–64

22. Levental I, Lyman E. 2022. Regulation of membrane protein structure and function by their lipid nano-environment. *Nat. Rev. Mol. Cell Biol.* 24:107–22

23. Tikku S, Epshtein Y, Collins H, Travis AJ, Rothblat GH, Levitan I. 2007. Relationship between Kir2.1/Kir2.3 activity and their distributions between cholesterol-rich and cholesterol-poor membrane domains. *Am. J. Physiol. Cell Physiol.* 293(1):440–50

24. Huang SK, Almurad O, Pejana RJ, Morrison ZA, Pandey A, et al. 2022. Allosteric modulation of the adenosine A2A receptor by cholesterol. *eLife* 11:73901

25. Bogdanov M, Heacock PN, Dowhan W. 2002. A polytopic membrane protein displays a reversible topology dependent on membrane lipid composition. *EMBO J.* 21(9):2107–16

26. Tang Y, Xia H, Li D. 2018. Membrane phospholipid biosynthesis in bacteria. In *Advances in Membrane Proteins: Part I: Mass Processing and Transportation*, ed. Y Cao, pp. 77–119. Singapore: Springer

27. Mantsch HH, McElhaney RN. 1991. Phospholipid phase transitions in model and biological membranes as studied by infrared spectroscopy. *Chem. Phys. Lipids* 57(2–3):213–26

28. Silvestro L, Axelsen PH. 1998. Infrared spectroscopy of supported lipid monolayer, bilayer, and multibilayer membranes. *Chem. Phys. Lipids* 96(1–2):69–80

29. Zhao W, Moilanen DE, Fenn EE, Fayer MD. 2008. Water at the surfaces of aligned phospho-lipid multibilayer model membranes probed with ultrafast vibrational spectroscopy. *J. Am. Chem. Soc.* 130(42):13927–37

30. Volkov VV, Palmer DJ, Righini R. 2007. Distinct water species confined at the interface of a phospholipid membrane. *Phys. Rev. Lett.* 99(7):078302

31. Binder H. 2007. Water near lipid membranes as seen by infrared spectroscopy. *Eur. Biophys. J.* 36(4–5):265–79

32. Perakis F, De Marco L, Shalit A, Tang F, Kann ZR, et al. 2016. Vibrational spectroscopy and dynamics of water. *Chem. Rev.* 116(13):7590–607

33. Goñi FM, Arrondo JLR. 1986. A study of phospholipid phosphate groups in model membranes by Fourier transform infrared spectroscopy. *Faraday Discuss. Chem. Soc.* 81:117–26

34. Arrondo JLR, Goñi FM, Macarulla JM. 1984. Infrared spectroscopy of phosphatidylcholines in aqueous suspension a study of the phosphate group vibrations. *Biochim. Biophys. Acta* 794(1):165–68

35. Hübner W, Blume A. 1998. Interactions at the lipid-water interface. *Chem. Phys. Lipids* 96(1–2):99–123
36. Flanagan JC, Valentine ML, Baiz CR. 2020. Ultrafast dynamics at lipid-water interfaces. *Acc. Chem. Res.* 53(9):1860–68
37. Mendelsohn R, Davies MA, Brauner JW, Schuster HF, Dluhy RA. 1989. Quantitative determination of conformational disorder in the acyl chains of phospholipid bilayers by infrared spectroscopy. *Biochemistry* 28(22):8934–39
38. Tumbic GW, Hossan MY, Thielges MC. 2021. Protein dynamics by infrared spectroscopy. *Annu. Rev. Anal. Chem.* 14:229–321
39. Mukherjee P, Kass I, Arkin I, Zanni MT. 2006. Picosecond dynamics of a membrane protein revealed by 2D IR. *PNAS* 103(10):3528–33
40. Arsov Z, Quaroni L. 2007. Direct interaction between cholesterol and phosphatidylcholines in hydrated membranes revealed by ATR-FTIR spectroscopy. *Chem. Phys. Lipids* 150(1):35–48
41. Ludlam CFC, Arkin IT, Liu XM, Rothman MS, Rath P, et al. 1996. Fourier transform infrared spectroscopy and site-directed isotope labeling as a probe of local secondary structure in the transmembrane domain of phospholamban. *Biophys. J.* 70(4):1728–36
42. Arsov Z. 2015. Long-range lipid-water interaction as observed by ATR-FTIR spectroscopy. In *Membrane Hydration: The Role of Water in the Structure and Function of Biological Membranes*, ed. EA Disalvo, pp. 127–59. Cham, Switz.: Springer
43. Edington SC, Flanagan JC, Baiz CR. 2016. An empirical IR frequency map for ester C=O stretching vibrations. *J. Phys. Chem. A* 120(22):3888–96
44. Valentine ML, Waterland MK, Fathizadeh A, Elber R, Baiz CR. 2021. Interfacial dynamics in lipid membranes: the effects of headgroup structures. *J. Phys. Chem. B* 125(5):1343–50
45. Guerin AC, Riley K, Rupnik K, Kuroda DG. 2016. Determining the energetics of the hydrogen bond through FTIR: a hands-on physical chemistry lab experiment. *J. Chem. Educ.* 93(6):1124–29
46. Lewis RNAH, McElhaney RN. 2013. Membrane lipid phase transitions and phase organization studied by Fourier transform infrared spectroscopy. *Biochim. Biophys. Acta Biomembr.* 1828(10):2347–58
47. Valentine ML, Cardenas AE, Elber R, Baiz CR. 2020. Calcium-lipid interactions observed with isotope-edited infrared spectroscopy. *Biophys. J.* 118(11):2694–702
48. Hamm P, Zanni M. 2011. *Concepts and Methods of 2D Infrared Spectroscopy*. New York: Cambridge Univ. Press
49. Flanagan JC, Valentine ML, Baiz CR. 2020. Ultrafast dynamics at lipid−water interfaces. *Acc. Chem. Res.* 53(9):1860–68
50. Fayer MD. 2009. Dynamics of liquids, molecules, and proteins measured with ultrafast 2D IR vibrational echo chemical exchange spectroscopy. *Annu. Rev. Phys. Chem.* 60:21–38
51. Fayer MD. 2013. *Ultrafast Infrared Vibrational Spectroscopy*. Boca Raton, FL: Taylor & Francis
52. Kwak K, Park S, Finkelstein IJ, Fayer MD. 2007. Frequency-frequency correlation functions and apodization in two-dimensional infrared vibrational echo spectroscopy: a new approach. *J. Chem. Phys.* 127(12):124503
53. Kwac K, Cho M. 2003. Molecular dynamics simulation study of N-methylacetamide in water. II. Two-dimensional infrared pump-probe spectra. *J. Chem. Phys.* 119(4):2256–63
54. Eaves JD, Loparo JJ, Fecko CJ, Roberts ST, Tokmakoff A, Geissler PL. 2005. Hydrogen bonds in liquid water are broken only fleetingly. *PNAS* 102(37):13019–22
55. Lazonder K, Pshenichnikov MS, Wiersma DA. 2006. Easy interpretation of optical two-dimensional correlation spectra. *Opt. Lett.* 31(22):3354–56
56. Hamm P, Zanni M. 2011. *Concepts and Methods of 2D Infrared Spectroscopy*. New York: Cambridge Univ. Press
57. Valentine ML, Waterland MK, Fathizadeh A, Elber R, Baiz CR. 2021. Interfacial dynamics in lipid membranes: the effects of headgroup structures. *J. Phys. Chem. B* 125(5):1343–50
58. Stevenson P, Tokmakoff A. 2017. Ultrafast fluctuations of high amplitude electric fields in lipid membranes. *J. Am. Chem. Soc.* 139(13):4743–52
59. Kel O, Tamimi A, Thielges MC, Fayer MD. 2013. Ultrafast structural dynamics inside planar phospholipid multibilayer model cell membranes measured with 2D IR spectroscopy. *J. Am. Chem. Soc.* 135(30):11063–74

60. Edington SC, Halling DB, Bennett SM, Middendorf TR, Aldrich RW, Baiz CR. 2019. Non-additive effects of binding site mutations in calmodulin. *Biochemistry* 58(24):2730–39

61. Liu S, Featherston ER, Cotruvo JA, Baiz CR. 2021. Lanthanide-dependent coordination interactions in lanmodulin: a 2D IR and molecular dynamics simulations study. *Phys. Chem. Chem. Phys.* 23(38):21690–700

62. Valentine ML, Al-Mualem ZA, Baiz CR. 2021. Pump slice amplitudes: a simple and robust method for connecting two-dimensional infrared and Fourier transform infrared spectra. *J. Phys. Chem. A* 125(29):6498–504

63. Kwak K, Park S, Finkelstein IJ, Fayer MD. 2007. Frequency-frequency correlation functions and apodization in two-dimensional infrared vibrational echo spectroscopy: a new approach. *J. Chem. Phys.* 127(12):124503

64. Nandi N, Bhattacharyya K, Bagchi B. 2000. Dielectric relaxation and solvation dynamics of water in complex chemical and biological systems. *Chem. Rev.* 100(6):2013–45

65. Lopez CF, Nielsen SO, Klein ML, Moore PB. 2004. Hydrogen bonding structure and dynamics of water at the dimyristoylphosphatidylcholine lipid bilayer surface from a molecular dynamics simulation. *J. Phys. Chem. B* 108(21):6603–10

66. Valentine ML, Cardenas AE, Elber R, Baiz CR. 2018. Physiological calcium concentrations slow dynamics at the lipid-water interface. *Biophys. J.* 115(8):1541–51

67. Flanagan JC, Cardenas AE, Baiz CR. 2020. Ultrafast spectroscopy of lipid-water interfaces: Transmembrane crowding drives H-bond dynamics. *J. Phys. Chem. Lett.* 11(10):4093–98

68. Nihonyanagi S, Yamaguchi S, Tahara T. 2017. Ultrafast dynamics at water interfaces studied by vibrational sum frequency generation spectroscopy. *Chem. Rev.* 117(16):10665–93

69. Inoue KI, Nihonyanagi S, Singh PC, Yamaguchi S, Tahara T. 2015. 2D heterodyne-detected sum frequency generation study on the ultrafast vibrational dynamics of H_2O and HOD water at charged interfaces. *J. Chem. Phys.* 142(21):212431

70. Xiong W, Laaser JE, Mehlenbacher RD, Zanni MT. 2011. Adding a dimension to the infrared spectra of interfaces using heterodyne detected 2D sum-frequency generation (HD 2D SFG) spectroscopy. *PNAS* 108(52):20902–7

71. Ghosh A, Smits M, Bredenbeck J, Bonn M. 2007. Membrane-bound water is energetically decoupled from nearby bulk water: an ultrafast surface-specific investigation. *J. Am. Chem. Soc.* 129(31):9608–9

72. Singh PC, Inoue KI, Nihonyanagi S, Yamaguchi S, Tahara T. 2016. Femtosecond hydrogen bond dynamics of bulk-like and bound water at positively and negatively charged lipid interfaces revealed by 2D HD-VSFG spectroscopy. *Angew. Chem. Int. Ed.* 55(36):10621–25

73. Singh PC, Ahmed M, Nihonyanagi S, Yamaguchi S, Tahara T. 2022. DNA-induced reorganization of water at model membrane interfaces investigated by heterodyne-detected vibrational sum frequency generation spectroscopy. *J. Phys. Chem. B* 126(4):840–46

74. Sarkar S, Singh PC. 2023. Selective action of antimalarial hydroxychloroquine on the packing of phospholipids and interfacial water associated with lysosomal model membranes: a vibrational sum frequency generation study. *Langmuir* 39(6):2435–43

75. Kundu A, Yamaguchi S, Tahara T. 2014. Evaluation of pH at charged lipid/water interfaces by heterodyne-detected electronic sum frequency generation. *J. Phys. Chem. Lett.* 5(4):762–66

76. Hua W, Verreault D, Allen HC. 2015. Solvation of calcium-phosphate headgroup complexes at the DPPC/aqueous interface. *ChemPhysChem* 16(18):3910–15

77. Ataka K, Kottke T, Heberle J. 2010. Thinner, smaller, faster: IR techniques to probe the functionality of biological and biomimetic systems. *Angew. Chem. Int. Ed.* 49(32):5416–24

78. Chuntonov L, Rubtsov IV. 2020. Surface-enhanced ultrafast two-dimensional vibrational spectroscopy with engineered plasmonic nano-antennas. *J. Chem. Phys.* 153:050902

79. Kusa F, Morichika I, Takegami A, Ashihara S. 2017. Enhanced ultrafast infrared spectroscopy using coupled nanoantenna arrays. *Opt. Express* 25(11):12896–907

80. Huck C, Neubrech F, Vogt J, Toma A, Gerbert D, et al. 2014. Surface-enhanced infrared spectroscopy using nanometer-sized gaps. *ACS Nano* 8(5):4908–14

81. Neubrech F, Huck C, Weber K, Pucci A, Giessen H. 2017. Surface-enhanced infrared spectroscopy using resonant nanoantennas. *Chem. Rev.* 117(7):5110–45

82. Osawa M, Ataka KI, Ikeda M, Uchihara H, Nanba R. 1991. Surface enhanced infrared absorption spectroscopy: mechanism and application to trace analysis. *Anal. Sci.* 7:503–6

83. Osawa M, Ataka K, Yoshii K, Yotsuyanagi T. 1993. Surface-enhanced infrared ATR spectroscopy for in situ studies of electrode/electrolyte interfaces. *J. Electron Spectros. Relat. Phenom.* 64–65:371–79

84. Osawa M. 1997. Dynamic processes in electrochemical reactions studied by surface-enhanced infrared absorption spectroscopy (SEIRAS). *Bull. Chem. Soc. Jpn.* 70(12):2861–80

85. Tseng C, Pennathur AK, Blauth D, Salazar N, Dawlaty JM. 2023. Direct determination of plasmon enhancement factor and penetration depths in surface enhanced IR absorption spectroscopy. *Langmuir* 39(9):3179–84

86. Maroun F, Ozanam F, Chazalviel JN, Theiß W. 1999. In situ infrared investigation of metals electrodeposited for SEIRAS. *Vib. Spectrosc.* 19(2):193–98

87. Prokopec V, Dendisová-Vyškovská M, Kokaislová A, Čejková J, Člupek M, Matějka P. 2011. Spectroscopic study of SERS- and SEIRA-activity of copper large-scaled surface substrates prepared by electrochemical deposition: What is the role of oxidation-reduction cycle treatment? *J. Mol. Struct.* 993(1–3):410–19

88. Osawa M, Ikeda M. 1991. Surface-enhanced infrared absorption of p-nitrobenzoic acid deposited on silver island films: contributions of electromagnetic and chemical mechanisms. *J. Phys. Chem.* 95(24):9914–19

89. Hartstein A, Kirtley JR, Tsang JC. 1980. Enhancement of the infrared absorption from molecular monolayers with thin metal overlayers. *Phys. Rev. Lett.* 45(3):201–4

90. Jensen TR, Van Duyne RP, Johnson SA, Maroni VA. 2000. Surface-enhanced infrared spectroscopy: a comparison of metal island films with discrete and nondiscrete surface plasmons. *Appl. Spectrosc.* 54(3):371–77

91. Killian M, Villa-Aleman E, Sun Z, Crittenden S, Leverette C. 2011. Dependence of surface-enhanced infrared absorption (SEIRA) enhancement and spectral quality on the choice of underlying substrate: a closer look at silver (Ag) films prepared by physical vapor deposition (PVD). *Appl. Spectrosc.* 65(3):272–83

92. Hatta A, Suzuki Y, Suëtaka W. 1984. Infrared absorption enhancement of monolayer species on thin evaporated Ag films by use of a Kretschmann configuration: evidence for two types of enhanced surface electric fields. *Appl. Phys. A* 35(3):135–40

93. Bao W-J, Li J, Li J, Zhang Q-W, Liu Y, et al. 2018. Au/ZnSe-based surface enhanced infrared absorption spectroscopy as a universal platform for bioanalysis. *Anal. Chem.* 90(6):3842–48

94. Pennathur AK, Tseng C, Salazar N, Dawlaty JM. 2022. Controlling water delivery to an electrochemical interface with surfactants. *J. Am. Chem. Soc.* 145(4):2421–29

95. Wu L, Zeng L, Jiang X. 2015. Revealing the nature of interaction between graphene oxide and lipid membrane by surface-enhanced infrared absorption spectroscopy. *J. Am. Chem. Soc.* 137(32):10052–55

96. Burdach K, Dziubak D, Sek S. 2022. Surface-enhanced infrared absorption spectroscopy (SEIRAS) to probe interfacial water in floating bilayer lipid membranes (fBLMs). In *Membrane Lipids: Methods and Protocols*, ed. CG Cranfield, pp. 199–207. New York: Springer US

97. Uchida T, Osawa M, Lipkowski J. 2014. SEIRAS studies of water structure at the gold electrode surface in the presence of supported lipid bilayer. *J. Electroanal. Chem.* 716:112–19

98. Ataka K, Baumann A, Chen JL, Redlich A, Heberle J, Schlesinger R. 2022. Monitoring the progression of cell-free expression of microbial rhodopsins by surface enhanced IR spectroscopy: resolving a branch point for successful/unsuccessful folding. *Front. Mol. Biosci.* 9:929285

99. Lipkowski J. 2014. Biomimetic membrane supported at a metal electrode surface: a molecular view. In *Advances in Planar Lipid Bilayers and Liposomes*, Vol. 20, ed. A Iglič, CV Kulkarni, pp. 1–49. Amsterdam: Elsevier

100. Ferhan AR, Yoon BK, Park S, Sut TN, Chin H, et al. 2019. Solvent-assisted preparation of supported lipid bilayers. *Nat. Protoc.* 14(7):2091–118

101. Ataka K, Drauschke J, Stulberg V, Koksch B, Heberle J. 2022. pH-induced insertion of pHLIP into a lipid bilayer: in-situ SEIRAS characterization of a folding intermediate at neutral pH. *Biochim. Biophys. Acta Biomembr.* 1864(6):183873

102. Birdsall ER, Petti MK, Saraswat V, Ostrander JS, Arnold MS, Zanni MT. 2021. Structure changes of a membrane polypeptide under an applied voltage observed with surface-enhanced 2D IR spectroscopy. *J. Phys. Chem. Lett.* 12(7):1786–92

103. Yamakata A, Uchida T, Kubota J, Osawa M. 2006. Laser-induced potential jump at the electrochemical interface probed by picosecond time-resolved surface-enhanced infrared absorption spectroscopy. *J. Phys. Chem. B* 110(13):6423–27

104. Paleček D, Tek G, Lan J, Iannuzzi M, Hamm P. 2018. Characterization of the platinum-hydrogen bond by surface-sensitive time-resolved infrared spectroscopy. *J. Phys. Chem. Lett.* 9(6):1254–59

105. Kraack JP, Hamm P. 2016. Vibrational ladder-climbing in surface-enhanced, ultrafast infrared spectroscopy. *Phys. Chem. Chem. Phys.* 18(24):16088–93

106. Lotti D, Hamm P, Kraack JP. 2016. Surface-sensitive spectro-electrochemistry using ultrafast 2D ATR IR spectroscopy. *J. Phys. Chem. C* 120(5):2883–92

107. Yang N, Ryan MJ, Son M, Mavric A, Zanni MT. 2023. Voltage-dependent FTIR and 2D infrared spectroscopies within the electric double layer using a plasmonic and conductive electrode. *J. Phys. Chem. B* 127:2083–91

108. Kraack JP, Hamm P. 2017. Surface-sensitive and surface-specific ultrafast two-dimensional vibrational spectroscopy. *Chem. Rev.* 117(16):10623–64

109. Kraack JP, Lotti D, Hamm P. 2015. Surface-enhanced, multi-dimensional attenuated total reflectance spectroscopy. *Proc. SPIE* 9549:95490S

110. Sponholtz MR, Senning EN. 2021. The pleckstrin homology domain of PLCδ1 exhibits complex dissociation properties at the inner leaflet of plasma membrane sheets. *ACS Chem. Neurosci.* 12(12):2072–78

111. Lee E, You X, Baiz CR. 2022. Interfacial dynamics in inverted-headgroup lipid membranes. *J. Chem. Phys.* 156(7):075102

112. Hsieh CS, Okuno M, Hunger J, Backus EHG, Nagata Y, Bonn M. 2014. Aqueous heterogeneity at the air/water interface revealed by 2D-HD-SFG spectroscopy. *Angew. Chem. Int. Ed.* 53(31):8146–49

113. Cerbón J, Calderón V. 1991. Changes of the compositional asymmetry of phospholipids associated to the increment in the membrane surface potential. *Biochim. Biophys. Acta Biomembr.* 1067(2):139–44

114. Cherniavskyi YK, Fathizadeh A, Elber R, Tieleman DP. 2020. Computer simulations of a heterogeneous membrane with enhanced sampling techniques. *J. Chem. Phys.* 153(14):144110

115. Bennett WFD, Tieleman DP. 2013. Computer simulations of lipid membrane domains. *Biochim. Biophys. Acta Biomembr.* 1828(8):1765–76

116. Fábián B, Vattulainen I, Javanainen M. 2023. Protein crowding and cholesterol increase cell membrane viscosity in a temperature dependent manner. *J. Chem. Theory Comput.* 19(9):2630–43

117. Dickson CJ, Walker RC, Gould IR. 2022. Lipid21: complex lipid membrane simulations with AMBER. *J. Chem. Theory Comput.* 18(3):1726–36

118. Baiz CR, Błasiak B, Bredenbeck J, Cho M, Choi JH, et al. 2020. Vibrational spectroscopic map, vibrational spectroscopy, and intermolecular interaction. *Chem. Rev.* 120(15):7152–218

119. Baiz CR, Reppert M, Tokmakoff A. 2013. Amide I two-dimensional infrared spectroscopy: methods for visualizing the vibrational structure of large proteins. *J. Phys. Chem. A* 117(29):5955–61

120. You X, Lee E, Xu C, Baiz CR. 2021. Molecular mechanism of cell membrane protection by sugars: a study of interfacial H-bond networks. *J. Phys. Chem. Lett.* 12(39):9602–7

121. Tang F, Ohto T, Sun S, Rouxel JR, Imoto S, et al. 2020. Molecular structure and modeling of water-air and ice-air interfaces monitored by sum-frequency generation. *Chem. Rev.* 120(8):3633–67

122. Fathizadeh A, Elber R. 2018. A mixed alchemical and equilibrium dynamics to simulate heterogeneous dense fluids: illustrations for Lennard-Jones mixtures and phospholipid membranes. *J. Chem. Phys.* 149(7):72325

123. Mori T, Miyashita N, Im W, Feig M, Sugita Y. 2016. Molecular dynamics simulations of biological membranes and membrane proteins using enhanced conformational sampling algorithms. *Biochim. Biophys. Acta Biomembr.* 1858(7):1635–51

124. Marrink SJ, Corradi V, Souza PCT, Ingólfsson HI, Tieleman DP, Sansom MSP. 2019. Computational modeling of realistic cell membranes. *Chem. Rev.* 119(9):6184–226

125. Antila HS, Kav B, Miettinen MS, Martinez-Seara H, Jungwirth P, Ollila OHS. 2022. Emerging era of biomolecular membrane simulations: automated physically-justified force field development and quality-evaluated databanks. *J. Phys. Chem. B* 2022:4169–83

126. Lyubartsev AP, Rabinovich AL. 2016. Force field development for lipid membrane simulations. *Biochim. Biophys. Acta Biomembr.* 1858(10):2483–97

127. Yu Y, Venable RM, Thirman J, Chatterjee P, Kumar A, et al. 2023. Drude polarizable lipid force field with explicit treatment of long-range dispersion: parametrization and validation for saturated and monounsaturated zwitterionic lipids. *J. Chem. Theory Comput.* 19(9):2590–605

128. Tempra C, Ollila OHS, Javanainen M. 2022. Accurate simulations of lipid monolayers require a water model with correct surface tension. *J. Chem. Theory Comput.* 18(3):1862–69

129. Melcr J, Ferreira TM, Jungwirth P, Ollila OHS. 2020. Improved cation binding to lipid bilayers with negatively charged POPS by effective inclusion of electronic polarization. *J. Chem. Theory Comput.* 16(1):738–48

130. Mohammad-Aghaie D, Bresme F. 2016. Force-field dependence on the liquid-expanded to liquid-condensed transition in DPPC monolayers. *Mol. Simul.* 42(5):391–97

131. Klauda JB, Wu X, Pastor RW, Brooks BR. 2007. Long-range Lennard-Jones and electrostatic interactions in interfaces: application of the isotropic periodic sum method. *J. Phys. Chem. B* 111(17):4393–400

132. Wu X, Brooks BR. 2019. The homogeneity condition: a simple way to derive isotropic periodic sum potentials for efficient calculation of long-range interactions in molecular simulation. *J. Chem. Phys.* 150(21):214109

133. Yu Y, Krämer A, Venable RM, Brooks BR, Klauda JB, Pastor RW. 2021. CHARMM36 lipid force field with explicit treatment of long-range dispersion: parametrization and validation for phosphatidylethanolamine, phosphatidylglycerol, and ether lipids. *J. Chem. Theory Comput.* 17(3):1581–95

134. Ingolfsson HI, Neale C, Carpenter TS, Shrestha R, Lopez CA, et al. 2022. Machine learning-driven multiscale modeling reveals lipid-dependent dynamics of RAS signaling proteins. *PNAS* 119(1):e2113297119

135. Walter V, Ruscher C, Benzerara O, Marques CM, Thalmann F. 2020. A machine learning study of the two states model for lipid bilayer phase transitions. *Phys. Chem. Chem. Phys.* 22(34):19147–54

136. Roy S, Gruenbaum SM, Skinner JL. 2014. Theoretical vibrational sum-frequency generation spectroscopy of water near lipid and surfactant monolayer interfaces. *J. Chem. Phys.* 141(18):18C502

137. Pieniazek PA, Tainter CJ, Skinner JL. 2011. Surface of liquid water: three-body interactions and vibrational sum-frequency spectroscopy. *J. Am. Chem. Soc.* 133(27):10360–63

138. Ballout F, Krassen H, Kopf I, Ataka K, Bründermann E, et al. 2011. Scanning near-field IR microscopy of proteins in lipid bilayers. *Phys. Chem. Chem. Phys.* 13(48):21432–36

139. Xu XG, Rang M, Craig IM, Raschke MB. 2012. Pushing the sample-size limit of infrared vibrational nanospectroscopy: from monolayer toward single molecule sensitivity. *J. Phys. Chem. Lett.* 3(13):1836–41

140. Berweger S, Nguyen DM, Muller EA, Bechtel HA, Perkins TT, Raschke MB. 2013. Nano-chemical infrared imaging of membrane proteins in lipid bilayers. *J. Am. Chem. Soc.* 135(49):18292–95

141. Govyadinov AA, Mastel S, Golmar F, Chuvilin A, Carney PS, Hillenbrand R. 2014. Recovery of permittivity and depth from near-field data as a step toward infrared nanotomography. *ACS Nano* 8(7):6911–21

142. Arkin IT. 2006. Isotope-edited IR spectroscopy for the study of membrane proteins. *Curr. Opin. Chem. Biol.* 10(5):394–401

143. Decatur SM. 2006. Elucidation of residue-level structure and dynamics of polypeptides via isotope-edited infrared spectroscopy. *Acc. Chem. Res.* 39(3):169–75

144. Gasse P, Stensitzki T, Mai-Linde Y, Linker T, Müller-Werkmeister HM. 2023. 2D-IR spectroscopy of carbohydrates: characterization of thiocyanate-labeled β-glucose in $CHCl_3$ and H_2O. *J. Chem. Phys.* 158(14):145101

145. Van Wilderen LJGW, Kern-Michler D, Müller-Werkmeister HM, Bredenbeck J. 2014. Vibrational dynamics and solvatochromism of the label SCN in various solvents and hemoglobin by time dependent IR and 2D-IR spectroscopy. *Phys. Chem. Chem. Phys.* 16(36):19643–53

146. Flores J, Brea RJ, Lamas A, Fracassi A, Salvador-Castell M, et al. 2022. Rapid and sequential dual oxime ligation enables de novo formation of functional synthetic membranes from water-soluble precursors. *Angew. Chem. Int. Ed.* 61(29):e202200549

147. Fracassi A, Podolsky KA, Pandey S, Xu C, Hutchings J, et al. 2023. Characterizing the self-assembly properties of monoolein lipid isosteres. *J. Phys. Chem. B* 127(8):1771–79

148. You X, Thakur N, Ray AP, Eddy MT, Baiz CR. 2022. A comparative study of interfacial environments in lipid nanodiscs and vesicles. *Biophys. Rep.* 2(3):1000066

149. Song W, Joshi H, Chowdhury R, Najem JS, Shen Y-X, et al. 2019. Artificial water channels enable fast and selective water permeation through water-wire networks. *Nat. Nanotechnol.* 15(1):73–79